Progress In Electromagnetics Research Letters, Vol. 105, 71–78, 2022

Extending the Absorption Frequency Band Using Twisted Configuration in the GHz Region

Pham V. Dien[1], Pham V. Hai[1], Vu M. Tu[1], Nguyen T. Thuy[1], Do H. Tung[2], Pham V. Vinh[1], and Tran M. Cuong[1, *]

Abstract—The electromagnetic wave perfect absorption of metamaterial is focused on by scientists currently. Conventional studies typically use a basic unit cell and then develop the entire structure in production. In this paper, we study and use a full-sized twisted metamaterial structure with the expectation that this structure will reveal outstanding advantages and possess excellent electromagnetic absorption properties. The structure of the twisted metamaterial consists of two coincident layers of cyclic lattice stacked on top of each other. When one lattice layer rotates at a specified angle relative to the other, it generates a new lattice configuration and increases the absorption of the structure. Therefore, the frequency band widens up to 6 GHz.

1. INTRODUCTION

New materials are becoming increasingly important in many scientific fields, and it is important to find new materials with better electromagnetic properties that respond to technological developments. In recent years, metamaterials (MTMs) with new electromagnetic properties generated by creating artificial configurations on metal and dielectric substrates have been studied and applied vigorously in practice as shown in telecommunications, energy harvesting technology, electromagnetic beam wave controlling, biomedical sensors, etc. [1–10]. In all kinds of MTMs, materials that completely absorb waves called absorbers play a crucial role and possess the most practical application potential. If the structure is reasonably designed, the absorber material can effectively absorb incident wave energy or can effectively control the characteristics of the incident wave as required by the application. Many international groups have presented simple and effective absorber structures to capture the electromagnetic waves in the GHz frequency band or have a broadband working bandwidth. The structures applied can be multi-layers [11–13], fractal [14], supercell base configuration [15, 16], defect generating structure [17], using new materials or asymmetrical structures [18–23]. These configurations are interesting but do not yet exploit the self-control of the elements on the surface of the full structure. In this paper, we introduce a new concept in which a new configuration is created based on the rotation of two coincident networks of circular disks. By arranging two cyclic lattices on a surface and then twisting the appropriate angles of either lattice, new configuration surfaces are formed with increased absorbance and extended working frequency bands. The appropriate angles are investigated to find the optimal configuration. The power loss density and the surface electric field density at the absorption band are also studied to provide explanations of the physical principle for the structure. This is a new approach, which has not been focused on in this field. Research in this area promises to provide an efficient and simple way to fabricate wideband wave absorber materials.

Received 12 April 2022, Accepted 8 July 2022, Scheduled 27 July 2022

* Corresponding author: Tran Manh Cuong (tmcuong0279@gmail.com).

[1] Faculty of Physics, Hanoi National University of Education, 136 Xuan Thuy, Cau Giay, Hanoi, Vietnam. [2] Institute of Physics, Vietnam Academy of Science and Technology, 18 Hoang Quoc Viet, Hanoi, Vietnam.

2. TWISTED ABSORBER STRUCTURES

2.1. Full-Size Circular Disc Structure

Firstly, we choose the unit cell (UC) of the structure by using a metal (copper) disk with a radius $r = 1\,\text{mm}$, conductivity $\sigma = 5,8.10^7\,\text{S/m}$ (Fig. 1). Then, for the sake of simplicity and suitability for the fabrication in the GHz scale with the size of several cm to several tens cm, a full-sized disk model is created from 137 UCs for the investigation (Fig. 1). The structural parameters such as thickness and radius of copper plate, dielectric layer thickness, and back copper layer thickness remain unchanged, and the distance between adjacent UCs is chosen as $d = 7.8\,\text{mm}$.

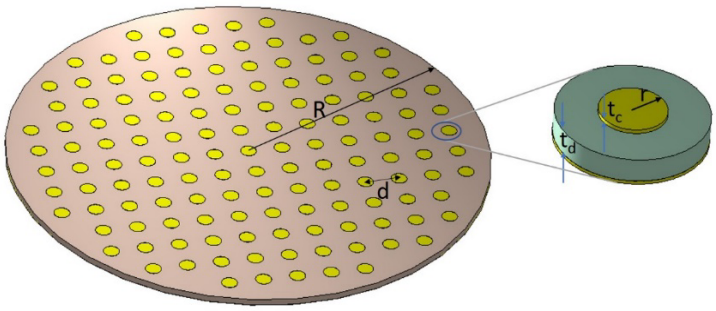

Figure 1. Full-sized structure of 137 UCs and the dimensions of one UC's disk.

2.2. Twisted Network Structure

A full structure of 137 UCs is designed as follows. It consists of three layers: Layer 1 is the bottom plate under the form of a circular copper disk with the thickness $t_c = 0.03\,\text{mm}$ and the radius $R = 55\,\text{mm}$. Layer 2 is the dielectric layer FR-4 with the same shape and size as the bottom copper disk, and the thickness of the dielectric layer is $t_d = 1.5\,\text{mm}$ with the relative dielectric constant $\varepsilon = 4.3$ and loss-tangent of 0.025. Layer 3 (top layer) consists of two coincident networks stacked, with each network consisting of 137 UCs as indicated in Session 2.1.

3. INVESTIGATIONS OF ROTATIONAL ANGLES

Our idea is to first design a full-sized structure of 137 UCs, then use two such identical surface lattices to coincide and rotate one lattice around the axis at the center of the entire structure by a rotation angle called α. This generates a new metasurface configuration. The values of the rotation angle α will be investigated to find the optimal configuration for the perfect absorption characteristic of the structure.

3.1. Rotational Angle 1°

Using CST Microwave studio software to simulate the structure of 137 unit-cells with the rotational angle between two circular disk networks of 1°, we obtained the results shown in Fig. 2. We also illustrate the absorption of a full-sized structure without rotation ($\alpha = 0$) for the comparison.

From the simulation results, with the application of a very small rotation angle of 1°, the absorption spectrum of the sample has significantly improved in comparison with the no-rotation angle case. Specifically, at the frequency band from 17.3 GHz to 17.7 GHz the absorption reaches above 95%.

3.2. Rotation Angle from 1.5° to 2.7°

With the rotation angle α from 1.5° to 2.7°, we specifically investigate the following angle values: 1.5°; 2°; 2.2°; 2.5°, and 2.7° (Fig. 3).

After performing the simulation, the results obtained for these five rotation angles show a broad absorption band, in which with a rotation angle of 1.5° GHz, the absorbance reaches over 90%, from

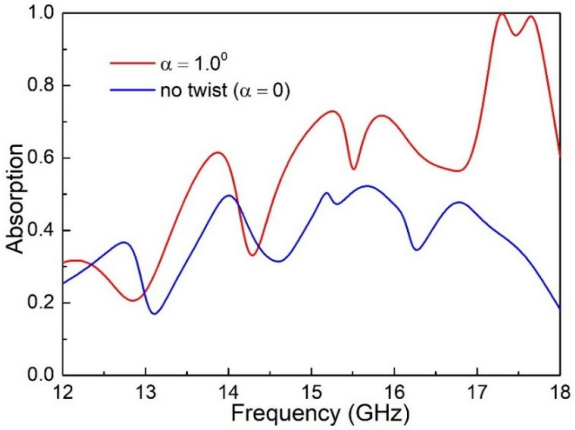

Figure 2. Absorption results of full structure of 137 UCs without and with rotational angle of 1°.

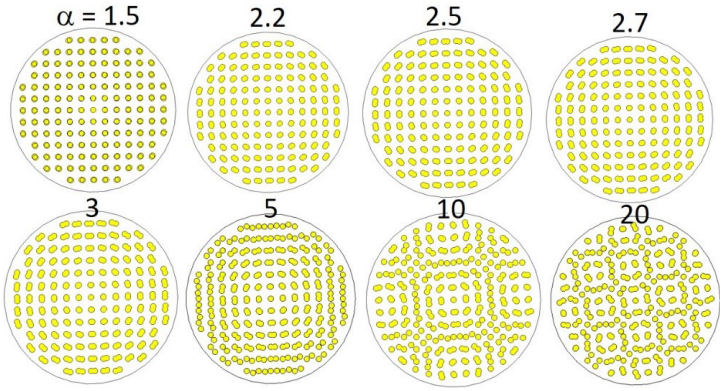

Figure 3. Eight "metamorphosis" structures with different rotation angles from 1.5° to 20°.

frequency $f = 14$ GHz to $f = 17.1$ GHz. With a rotation angle of 2°, there is an absorption band of 3.57 GHz, from frequency $f = 13.35$ GHz to $f = 16.92$ GHz. The rotation angle of 2.2° has a broad absorption band of 3.68 GHz, from frequency $f = 13.14$ GHz to $f = 16.82$ GHz. With both rotation angles above, the absorbance of the wideband is over 90%. The rotation angle of 2.5° has a broad absorption band of 3.86 GHz, from $f = 12.85$ GHz to $f = 16.75$ GHz, and the absorbance is over 95%. The angle of rotation 2.7° has a broad absorption band of 3.85 GHz, from frequency $f = 12.66$ GHz to $f = 16.52$ GHz, and the absorbance is over 85%. The results of absorbance according to the rotational angle are shown in Fig. 4(a). It should be emphasized that the case with the rotation angle of 2.5° has the highest absorption band and can be selected for further investigations. However, this is not the optimal case, and we just use it as a representative case. The cases with rotation angle from 1.5° to 3° all result in a wide absorption frequency band.

3.3. Angle of Rotation from 3° and Beyond

In the range of rotational angles from 3° and beyond, we investigate specifically for the values of angle 3°, angle 5°, 10°, and 20°, as shown in Fig. 3, and the absorption results are presented in Fig. 4(b). When the rotation angle increases to 3°, it is noticed that the width of the absorption bands is gradually decreasing compared to the case of swivel angles from 1.5° to 2.7°. Specifically, for a rotation angle of 3°, an absorption band with a width of 1.9 GHz and an absorption intensity over 90% appears (12 GHz–13.9 GHz). For a rotational angle of 5°, only an absorption band from 12 GHz to 13 GHz is observed with the absorption intensity reaching 90%. When the angle of rotation increases up to 10°, the wide absorbance band is not observed, and the absorption spectrum now exists only individual absorption

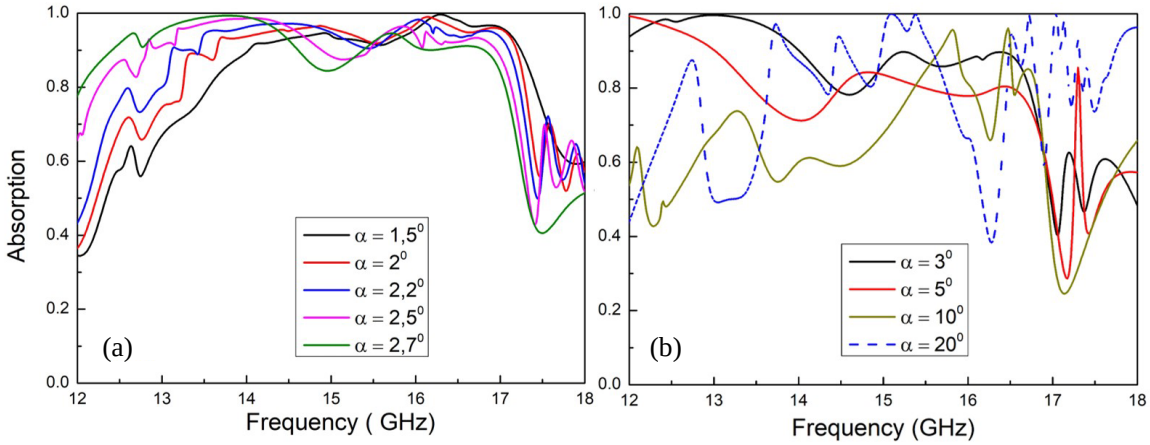

Figure 4. Results of the absorption with the rotational angle α from (a) 1.5° to 2.7° and (b) 3° to 20°.

peaks. Some peaks have high absorbance. For example, at frequency $f = 15.9$ GHz, the absorbance reaches 93.3%, and at frequency $f = 16.5$ GHz, the absorbance is 97.2%. When the rotation angle increases to 20°, the absorption spectrum is similar to that for the case of the rotation angle of 10°. Only the absorption peaks are observed, and broad absorption bands are not clearly formed.

In general, we can see the trend that when rapidly increasing the rotation angle α, the absorption band is no longer as optimal as for the cases of rotation angle below 3°. The absorption peaks, as well as the wide absorption band, tend to degrade.

4. FIELD DISTRIBUTIONS

To better understand the absorption mechanism of the structure when using different rotation angles and especially for structures with small rotation angles ($\alpha < 3°$) and broad absorption band structure, the surface electric field distribution and power loss density are studied at the frequency of 14 GHz (Fig. 5), for the three cases of rotation angles: $\alpha = 0°$ (no twist), $\alpha = 2.5°$ and $\alpha = 10°$. It is clear that, at 14 GHz, the structure with the rotation angle of 2.5° possesses the highest absorption energy

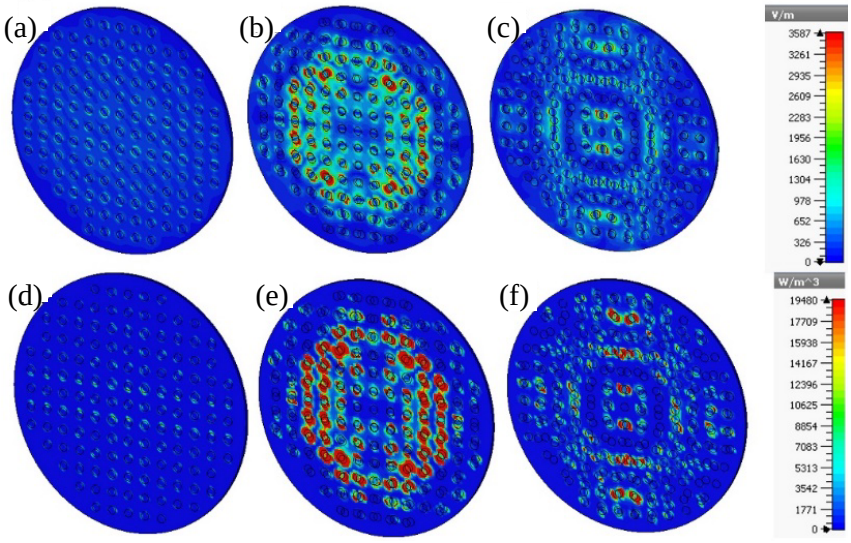

Figure 5. E fields (a)–(c) and power loss density (d)–(f) in the structure at 14 GHz: (a), (d) no twist structure; (b), (e) 2.5° rotation structure; and (c), (f): 10° rotation structure.

concentrated in the center region of the structure. The no-twist structure shows low absorption energy as well as low surface electric field density, and the 10° rotation structure has a higher absorption rate than the no-twist structure but is still much lower than that in the 2.5° rotation structure. This result indicates that the rotation angle of 2.5° case has created a metasurface for better energy confinement in the absorber. This reason also helps the absorption intensity of this structure to be much higher at 14 GHz. At other frequencies, similar observations are received but not presented here.

The surface current vectors are presented in Fig. 6. The observed structure is the configuration with the rotated angle of 2.5°. Two absorption frequencies are investigated, 14 GHz and 17 GHz, corresponding to the perfect absorption band of the structure. Surface currents are observed at the top metal disk lattice layer and the metal layer at the back of the structure. We can see that at these frequencies, antiparallel current systems are formed in the front layer and back of the structure, helping to generate the magnetic resonance and confine the energy of the incident wave, resulting in incoming wave complete absorption.

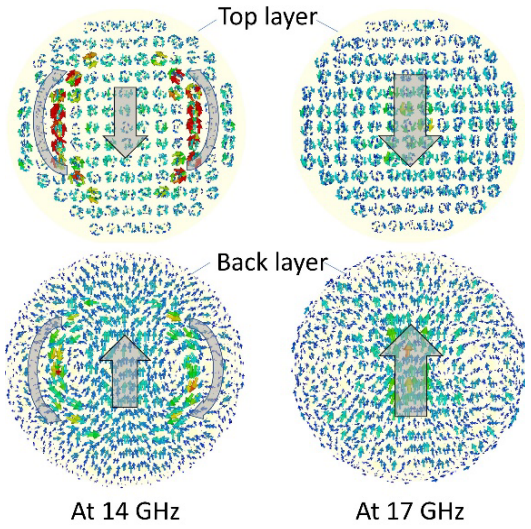

Figure 6. The surface currents observed at the frequencies of 14 GHz and 17 GHz for 2.5° rotation structure.

5. EQUIVALENT CIRCUIT MODEL FOR THE ANGLE BELOW 3°

To get a better insight into the physical nature of the absorption frequency spectrum, the equivalent electrical circuit of the full structure is shown in Fig. 7. The circuit consists of two main parts: the top layer and the backside of the sample. The surface consists of the arrays of capacitors C_i formed by neighboring disks in series with inductors L_i created by currents on the copper platters. Capacitor C_d is created by the dielectric layer separating the backside and top layer, and inductor L_b is created by the back copper layer. With the full structure studied, for the cases where the rotation angle is less than 3°, the relative area of the copper disks increases, causing L_i to increase, and the distance between them decreases, causing C_i to increase (Fig. 3, $\alpha = 1.5°$–3°). Therefore, the resonant frequency decreases ($\omega_i = \frac{1}{\sqrt{L_i C_i}}$), and the absorption frequency band tends to redshift, which is consistent with the results obtained in Fig. 4(a). For cases where the rotation angle increases gradually above 3° and up to 20°, the scenario becomes different as the relative area of the copper disks does not increase, but the top layer starts to form resonance cavities due to the combination of the copper plates (see cases of 10, 20 degrees, Fig. 4(b)). Therefore, the results become unstable, and this equivalent circuit model is not applicable.

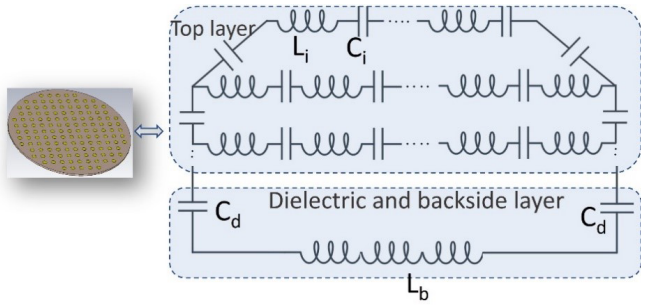

Figure 7. Equivalent circuit of the full-sized structure.

6. EXPERIMENTS

The fully no-twist structure and the structure with an optimal rotation angle of 2.5° were selected to fabricate for measurement (Fig. 8). The fabrication technique is standard photolithography. The Rohde & Schwarz ZNB20 (100 kHz to 20 GHz) vector network analyzer is used in measuring the absorbance through the surface reflection coefficient of the structure. During the measurement, two horn antennas working in the same working frequency range are used to generate the transmitting and receiving signals to the metasurface, with the incident angle near 0°. In Fig. 9, the measurement results show that, with

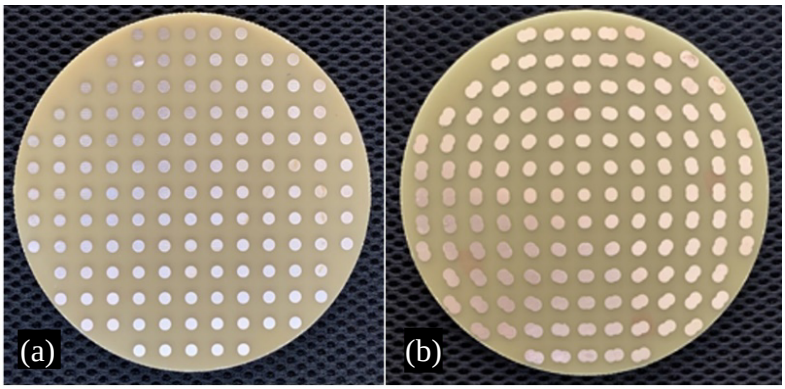

Figure 8. (a) The fully no-twist structure and (b) the structure with optimal rotation angle of 2.5°.

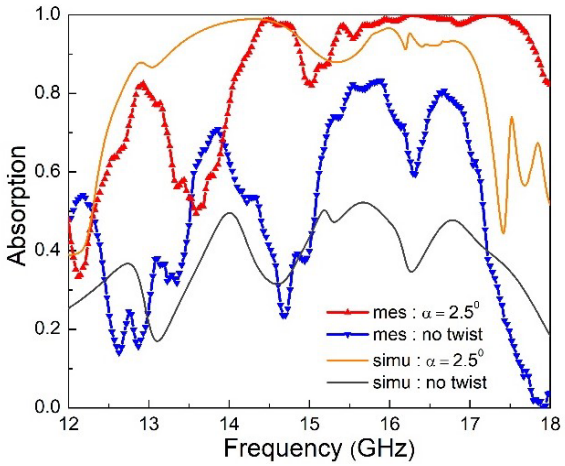

Figure 9. Comparison the simulation and experimental results of the absorber structures.

the optimal twisted structure, the absorption range is well above 95% from 14 to 18 GHz. The tendency of the measured results agrees with the simulated ones, but the discrepancies in the absorptivity and the frequency range are still observed. This can be explained by the imperfections of our prototype in fabrication; the installation of the horn antenna system, in reality, the 0° of the incident waves is difficult to set up due to the dimension of the horn antenna. Therefore, we set the incident angle near 5°, the inexact permittivity of the sample substrate, and the possibility that the simulation may not have considered all parameters of the system. This result confirms the accuracy of the study and the efficiency when applying the angle rotation technique of the two surface lattices for enhancing the working frequency band of the absorber.

7. CONCLUSIONS

Our proposed structure shows that with the metamaterial configurations generated from different rotation angles between the two identical networks, one can improve the electromagnetic properties of the structure. In this report, this method helps expand the working frequency band of the absorption structure by redistributing the surface electromagnetic density and creating the environment impedance matching. More broadly, this new concept of twisted metamaterial, obtained by breaking the traditional symmetry of metamaterial by rotating two identical lattices on the same plane, can help simplify the design process and extend the scope for devices and further applications of metamaterials.

ACKNOWLEDGMENT

This research is supported by the Ministry of Education and Training, Vietnam under grant number B2022-SPH-17.

REFERENCES

1. Pendry, J. B., D. Schurig, and D. R. Smith, "Controlling electromagnetic fields," *Science*, Vol. 312, 1780, 2006, https://doi.org/10.1126/science.1125907.
2. Luican, A., G. Li, A. Reina, J. Kong, R. R. Nair, K. S. Novoselov, A. K. Geim, and E. Y. Andrei, "Single-layer behavior and its breakdown in twisted graphene layers," *Phys. Rev. Lett.*, Vol. 106, 126802, 2011, https://doi.org/10.1103/PhysRevLett.106.126802.
3. Veselago, V. G., "The electrodynamics of substances with negative ε and μ," *Sov. Phys. Usp.*, Vol. 10, 509, 1968, https://doi.org/10.1070/PU1968v010n04ABEH003699.
4. Tran, M. C., T. T. Nguyen, T. H. Ho, and H. T. Do, "Creating a multiband perfect metamaterial absorber at K frequency band using defects in the structure," *J. Electron. Mater.*, Vol. 46, 413, 2017, http://dx.doi.org/10.1007/s11664-016-4863-0.
5. Wilbert, D. S., M. P. Hokmabadi, P. Kung, and S. M. Kim, "Equivalent-circuit interpretation of the polarization insensitive performance of THz metamaterial absorbers," *IEEE Trans. Terahertz Sci. Technol.*, Vol. 3, 846, 2013, https://doi.org/10.1109/TTHZ.2013.2285311.
6. Khanna, Y. and Y. K. Awasthi, "Ultra-thin wideband polarization-insensitive metasurface absorber for aviation technology," *J. Electron. Mater.*, Vol. 49, 6410–6416, 2020.
7. Carranza, I. E., G. James, G. John, and C. David, "Terahertz metamaterial absorbers implemented in CMOS technology for imaging applications: Scaling to large format focal plane arrays," *IEEE J. Sel. Top. Quantum Electron.*, Vol. 23, 4700508, 2017, 10.1109/JSTQE.2016.2630307.
8. Fatih, O. A., A. Olcay, O. Meliksah, K. Muharrem, A. Oguzhan, U. Emin, and S. Cumali, "Enhancement of image quality by using metamaterial inspired energy harvester," *Phys. Lett. A*, Vol. 384, No. 1, 126041, 2020, https://doi.org/10.1016/j.physleta.2019.126041.
9. Lei, Z., Y. W. Rui, D. B. Guo, T. W. Hao, M. Qian, Q. C. Xiao, and J. C. Tie, "Transmission-reflection-integrated multifunctional coding metasurface for full-space controls of electromagnetic waves," *Adv. Funct. Mater.*, Vol. 28, 33, 2018, https://doi.org/10.1002/adfm.201802205.

10. Banerjee, S., P. Dutta, A. K. Jha, P. R. Tripati, A. Srinivasulu, B. Appasani, and C. Ravariu, "A triple band highly sensitive refractive index sensor using terahertz metamaterial perfect absorber," *Progress In Electromagnetics Research M*, Vol. 107, 13–23, 2022.
11. Appasani, B., "An octaband temperature tunable terahertz metamaterial absorber using tapered triangular structures," *Progress In Electromagnetics Research Letters*, Vol. 95, 9–16, 2021.
12. Liu, S. H. Chen, and T. J. Cui, "A broadband terahertz absorber using multi-layer stacked bars," *Appl. Phys. Lett.*, Vol. 106, 151601, 2015, https://doi.org/10.1063/1.4918289.
13. Wang, B. X., X. Zhai, G. Z. Wang, W. Q. Huang, and L. L. Wang, "Design of a four-band and polarization-insensitive terahertz metamaterial absorber," *IEEE Photonics Journal*, Vol. 7, No. 1, 2014, https://doi.org/10.1109/JPHOT.2014.2381633.
14. Ma, J.-J., W. H. Tong, K. Shi, X.-Y. Cao, and B. Gong, "A broadband metamaterial absorber using fractal tree structure," *Progress In Electromagnetics Research Letters*, Vol. 49, 73–78, 2014.
15. Liu, Y., S. Gu, C. Luo, and X. Zhao, "Ultra-thin broadband metamaterial absorber," *Applied Physics A*, Vol. 108, 19, 2012, https://doi.org/10.1007/s00339-012-6936-0.
16. Cheng, Y. Z., W. Withayachumnankul, A. Upadhyay, D. Headland, Y. Nie, R. Z. Gong, M. Bhaskaran, S. Sriram, and D. Abbott, "Broadband and wide-angle reflective linear polarization," *Appl. Phys. Lett.*, Vol. 105, 181111, 2014, https://doi.org/10.1063/1.5116149.
17. Tran, S. T. and T. Q. H. Nguyen, "Defect induced co-polarization broadband metamaterial absorber," *AIP Advances*, Vol. 9, 055321, 2019, https://doi.org/10.1063/1.5097198.
18. He, S. and T. Chen, "Broadband THz absorbers with graphene-based anisotropic metamaterial films," *IEEE Trans. Terahertz Sci. Technol.*, Vol. 3, 757, 2013, Doi: 10.1109/TTHZ.2013.2283370.
19. Liu, X., Q. Zhang, and X. Cui, "Ultra-broadband polarization-independent wide-angle THz absorber based on plasmonic resonances in semiconductor square nut-shaped metamaterials," *Plasmonics*, Vol. 12, No. 4, 1137, 2017, https://doi.org/10.1007/s11468-016-0368-1.
20. Gu, S., B. Su, and X. Zhao, "Planar isotropic broadband metamaterial absorber," *J. Appl. Phys.*, Vol. 114, 163702, 2013, https://doi.org/10.1063/1.4826911.
21. Zhang, C., Q. Cheng, J. Yang, J. Zhao, and T. J. Cui, "Broadband metamaterial for optical transparency and microwave absorption," *Appl. Phys. Lett.*, Vol. 110, 143511, 2017, https://doi.org/10.1063/1.4979543.
22. Tang, J., Z. Xiao, K. Xu, X. Ma, and Z. Wang, "Polarization-controlled metamaterial absorber with extremely bandwidth and wide incidence angle," *Plasmonics*, Vol. 11, No. 5, 1393, 2016, https://doi.org/10.1007/s11468-016-01892.
23. Tran, M. C., H. P. Van, H. H. Tuan, T. T. Nguyen, H. T. Do, X. K. Bui, S. T. Bui, D. T. Le, T. L. Pham, and D. L. Vu, "Broadband microwave coding metamaterial absorbers," *Scientific Reports*, Vol. 10, 1810, 2020, https://doi.org/10.1038/s41598-020-58774-1.